Development of a Haptic Interface for Safe Human Robot Collaboration

Ioannis Iossifidis
IComputer Science Insitute, Ruhr West University of Applied Sciences, 45470 Mülheim an der Ruhr, Germany

Keywords: Haptic Interface, Artificial Skin, Direct Physical Interaction, Safe Collaboration.

Abstract: In the context of the increasing number of collaborative workplaces in industrial environments, where humans and robots sharing the same workplace, safety and intuitive interaction is a prerequisite. This means, that the robot can (1) have contact with his own body and the surrounding objects, (2) the motion of the robot can be corrected online by the human user just by touching his artificial skin or (3) interrupt the action in dangerous situations. In the current work we introduce a haptic interface (artificial skin) which is utilized to cover the arms of an anthropomorphic robotic assistant. The touched induced input of the artificial skin is interpreted and fed into the motor control algorithm to generate the desired motion and to avoid harm for human and machine.

1 INTRODUCTION

Modern production processes require a flexible use of the available resources and can not be covered efficiently by conventional rigid automation strategies. Work places in which man and machine collaborate sharing the same workspace in order to accomplish all of the required production steps contribute to a flexible design of production situation or a fast rearrangement at low costs. This implies that preprogrammed rigid machines should be replaced by autonomous robotic assistant, which can be instructed intuitively and used in a wide variety of production scenarios.

Precondition for the use of such systems is the warranty of the safety of the involved employees. The security-related situation are characterized by the occurrence of intentional or unintentional contacts between man and machine. Both need to be allowed but without the danger of harming humans or destroying the machines. We define this kind of interaction as direct physical interaction by means of haptic and other force/torque related sensors. In consequence the two strongly linked aspects of physical interaction and safety have to be tackled together by the design of appropriate haptic sensors, the context sensitive interoperation of contact forces and the control of accelerations and velocities of the manipulators.

In this work we introduce a haptic sensor providing the functionality of an artificial skin, detecting and measuring contact forces and it's position. The contact forces are interpreted and the sensorial output is fed into the motion planning of the robotic arm. In order to handle motion constraints during the manipulation task the geometric structure, described by the closed form solution of the invers kinematics, of the redundant robot arm is exploited.

In the following we describe the haptic sensor in detail and sketch the closed form solution of the invers kinematics of the robot arm in order to clarify how contact forces are mapped to the arm motion. Finally we describe the implementation and the experimental results in simulation and on the anthropomorphic robot Cora (Iossifidis et al., 2002).

2 TARGET SYSTEM

2.1 The Artificial Skin

The artificial skin, invented by the SIEMENS robotics group, is based on a conductive foam, with the main characteristic of changing conductivity property when pressure is applied. The changing resistant of the foam is utilized to measure the extend of the applied pressure and to design a sensor which can cover arbitrary bodies in order to provide a touch sensitive skin.

The sensor consists of two layers (two pads) of the foam, each of equipped with two parallel electrodes. The pads are arranged such that the electrodes are or-

Iossifidis I..
Development of a Haptic Interface for Safe Human Roobt Collaboration.
DOI: 10.5220/0004803400610066
In *Proceedings of the 4th International Conference on Pervasive and Embedded Computing and Communication Systems* (PECCS-2014), pages 61-66
ISBN: 978-989-758-000-0

Figure 1: Anthropomorphic robot CORA.

thogonal in order to calculate the position of the pressure point of the associated pressure measure.

The electrodes are connected to a sensor board equipped with A/D converters and a micro controller. The electrodes of the upper pad are connected to 5 V (one electrode to ground the other to 5 V) – if pressure is applied the voltage drops according to the pressure point. Both electrodes of the lower layer are connected to the micro controller, who generates a periodically varying voltage between 0 V and 5 V.

As soon a force is applied to the upper layer, the voltage of the lower layer tuned to the voltage of the upper layer according to the position of the pressure point. The read out of the complete unit provides us with a measure of the applied force and the position of the pressure point.

We have covered two of CORA's arm-modules with the artificial skin mounted on a cylindric silicon cuff (see figure 2). The advantage of the cylindric cuff is that the vector valued contact force is obtain directly from the scalar valued pressure measure. The direction of the contact force defines the motion direction of the related limb.

2.2 Robot CORA

CORA's body consists of a redundant seven DoF manipulator connected to a one DoF trunk which is fixed on the edge of a table (see figure 1). CORA can exploit the redundant eight DoF of the arm-trunk configuration that guarantees a high degree of flexibility with respect to manipulation tasks under external constraints. Grasping, for instance, is possible in the whole workspace choosing different arm postures without the necessity of changing the position or orientation of the end-effector. By turning the trunk joint, the robot can also change its configuration from right- to left-handed. The sensor equipment and the configuration of the joints in CORA's body and manipulator arm are anthropomorphic, which means that they are structurally similar to the human body.

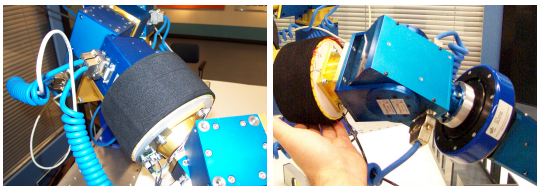

Figure 2: The figure depicts the cylindric cuffs with the artificial skin which cover the squared module on the upper arm (left) and the fore arm (right).

Two of CORA's arm-modules are covered with the artificial skin mounted on a cylindric silicon cuff (see figure 2). The advantage of the cylindric cuff is that a scalar pressure value can be interpreted directly as a force vector perpendicular to the cylinder's surface defining the direction in which the limb should be moved (for more details see (Iossifidis et al., 2002)).

2.3 Kinematics

2.3.1 Initial Configuration

The sketched structure models (in correspondence to humans) a one degree of freedom trunk, a one degree of freedom shoulder elevation/depression with an attached seven degree of freedom arm. The arm consisting of a rotating trunk, spherical shoulder and wrist joints, and an elbow joint, for a total of nine degrees of freedom. The reference configuration is show in Figure 3.

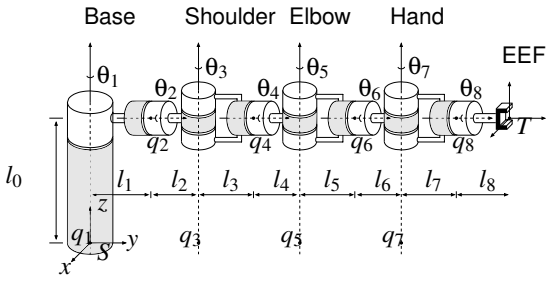

Figure 3: A total of eight revolute joints are ordered along the effector to simulate a human arm with trunk, shoulder, elbow and wrist.

The manipulator is composed of a series of *roll* and *pitch* joints. The combination of a *roll-pitch-roll-*

joint is functionally equivalent to a spherical three DoF joint like the human shoulder or wrist. Similar to the example above, the twists are determined as

$$\omega_1 = \omega_3 = \omega_5 = \omega_7 = \begin{bmatrix} 0 \\ 0 \\ 1 \end{bmatrix}, \quad \omega_2 = \omega_4 = \omega_6 = \omega_8 = \begin{bmatrix} 0 \\ 1 \\ 0 \end{bmatrix}.$$

Support points can be chosen as

$$q_i = \begin{bmatrix} 0 \\ \sum_{k=1}^{i-1} l_k \\ 0 \end{bmatrix} \qquad \text{for} \quad i = 1,3,5,7,$$

and

$$q_i = \begin{bmatrix} 0 \\ \sum_{k=1}^{i-1} l_k \\ l_0 \end{bmatrix} \qquad \text{for} \quad i = 2,4,6,8.$$

This yields the twist coordinates

$$\xi_1 = \begin{bmatrix} 0 \\ 0 \\ 0 \\ 0 \\ 0 \\ 1 \end{bmatrix}, \quad \xi_3 = \begin{bmatrix} l_1 + l_2 \\ 0 \\ 0 \\ 0 \\ 0 \\ 1 \end{bmatrix}, \quad \xi_4 = \begin{bmatrix} l_1 + l_2 + l_3 + l_4 \\ 0 \\ 0 \\ 0 \\ 0 \\ 1 \end{bmatrix},$$

$$\xi_7 = \begin{bmatrix} l_1 + l_2 + l_3 + l_4 + l_5 + l_6 \\ 0 \\ 0 \\ 0 \\ 0 \\ 1 \end{bmatrix}, \qquad \xi_{2,4,6,8} = \begin{bmatrix} l_0 \\ 0 \\ 0 \\ 0 \\ 0 \\ 1 \end{bmatrix}.$$

The transformation between the base and end-effector coordinate frames in reference configuration is

$$g_{st}(0) = \begin{bmatrix} I & \begin{pmatrix} 0 \\ \sum_{i=1}^{9} l_i \\ l_0 \end{pmatrix} \\ 0 & 1 \end{bmatrix}.$$

2.3.2 Forward Kinematics

The forward kinematics is calculated as the product of exponential. On the basis of the simple ways of representing and calculating rigid transformations (for detailed description see (Murray et al., 1994)), we can move on to describe the transformation to the end effector of an open chain manipulator, that is, a chain of n joints. For each joint, we define a joint twist ξ_i that models the motion of the subsequent part of the robot.

Let $g_{st}(0)$ be the transformation between the base frame S of the manipulator and the end effector, or tool frame T in the reference configuration, that is, when all joint angles[1] $\theta_1, \ldots, \theta_n$ are set to zero.

[1]By abusive convention, we refer to the amount of translation θ_k of a prismatic joint k as *angle*, too, in order to prevent cluttering up our language.

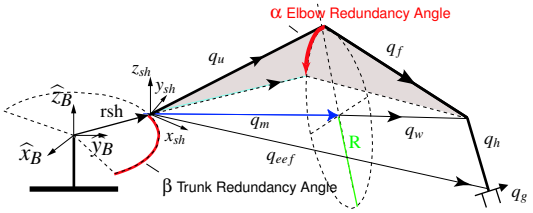

Figure 4: The figure depicts the kinematical structure and the associated coordinate systems of an multi redundant nine degree of freedom arm. α denotes the elbow angle, β denotes the trunk angle and γ the shoulder angle.

Now we want to know what happens to the end effector after we apply a rigid transformation by moving a joint. Starting at the base, we get to the end effector via $g_{st}(0)$, which we then move by applying the rigid transformation $e^{\hat{\xi}_i \theta_i}$. Combining these two transformation in the right order, we get

$$g_{st}(\theta) = e^{\hat{\xi}_i \theta_i} g_{st}(0).$$

Here $g_{st}(\theta)$ maps the center of the base frame to the position of the end effector in the new configuration with $\theta_i \neq 0$. Thinking the other way round, it returns the S-coordinates of a point that we specify in T-coordinates. So if we specify "0", we refer to the position of the end effector in the frame T centered at that point. Applying $g_{st}(\theta)$ returns the coordinates of that point in frame S, centered at the base. Thus, we can think of $g_{st}(\theta)$ as enabling us to specify a point in a moving frame T, and get back its position in the motionless frame S.

To do the same for a configuration in which several joints have moved, i.e. $\theta_i \neq 0$ for more than one i, we just have to apply the appropriate transformation in the right order. Conceptually speaking, we start at the end effector and go up the joints along the manipulator till we reach the base, moving each joint by the appropriate angle θ_i on the way. This yields

$$g_{st}(\theta) = e^{\hat{\xi}_1 \theta_1} \cdots e^{\hat{\xi}_n \theta_n} g_{st}(0) \qquad (1)$$

as the coordinate transformation from T to S in configuration $\theta = (\theta_1, \ldots, \theta_n)$.

Equation (1) is called the *product of exponentials* formula for the manipulator forward kinematics.

2.3.3 Closed Form Solution

For the solution of the overall system we assume that the shoulder is positioned due to the boundary condition determined by the object to be manipulated, like turning shoulder towards the object to extend it's workspace (distances to objects greater the the length of the arm) or to position the shoulder to an orientation that is orthogonal to the target direction (optimal

grasping position). The shoulder elevation/depression is utilized to satisfy additional constraints, like the avoidance of undesired configurations.

Given the shoulder position, which is determined by the trunk angle and the shoulder angle, the inverse kinematic mapping of the seven degree of freedom has to be derived with respect to shoulder coordinate system.

In the following we derive first the inverse kinematics of the seven degree of freedom, exploiting it's geometric properties, and describe how the null space motion can be utilized to satisfy constraints like obstacle avoidance and joint limits.

Inverse Kinematics. Based on the work of (Kreutz-Delgado et al., 1990) and (Hollerbach, 1984) the inverse kinematics problem for the eight degrees of freedom manipulator is solved in closed form. In the following derivation we denote the trunk angle with β (correspond to θ_1 in the initial configuration in figure 3).

We assume that the end effector position and hand orientation is determined by the object to be grasped and that the trunk angle β

will be choosen due to the boundary conditions and costraints of the given task. First we transform the given end effector position to the shoulder coordinate system by:

$$q'_{eef} = T^S_{sh} q_{eef}$$

with

$$T^S_{sh} = \begin{bmatrix} 1 & 0 & 0 & 0 \\ 0 & 1 & 0 & -(l_2+l_1) \\ 0 & 0 & 1 & -l_0 \\ 0 & 0 & 0 & 1 \end{bmatrix} \begin{bmatrix} \cos(-\theta_1) & -\sin(-\theta_1) & 0 & 0 \\ \sin(-\theta_1) & \cos(-\theta_1) & 0 & 0 \\ 0 & 0 & 1 & 0 \\ 0 & 0 & 0 & 1 \end{bmatrix}$$

beeing the homogeneous transformation.

Given the hand orientation θ_h (elevation) and ϕ_h (azimuth) and the tool point q'_{eef}, the vector q_h from the wrist to the hand reference tool-point (Fig. 4) is determined as

$$q_h = R_z(\phi_h) R_y(\theta_h) \hat{e}_y l_h \qquad (2)$$

where R_x, R_z denote rotation matrices around the z- and y-axes and l_h denotes the segment length.

The redundant degree of freedom is defined by the *redundancy circle*, the center

$$q_m = \frac{|q_u|^2 - |q_f|^2 + |q_w|^2}{2|q_w|^2} q_w \qquad (3)$$

of which lies on a ray pointing from the shoulder to the wrist joint. The spatial position of the elbow lies on this circle of radius r, with

$$r = \sqrt{|q_u|^2 - \left(\frac{|q_u|^2 - |q_f|^2 + |q_w|^2}{2|q_w|} \right)^2} \qquad (4)$$

Expressing the wrist vector, q_w, through two angles, ϕ_w and θ_w, the elbow position can be written as

$$q_u = (R_x(\phi_w) R_z(\theta_w) R_x(\alpha) \hat{e}_y)\, r + q_m \qquad (5)$$

where R_x and R_z are rotation matrices around the x- and the z-axis and the *redundancy angle* α characterizes the position of the elbow on the redundancy circle (Fig. 4). If α is specified, all limb vectors are known. A straightforward solution of the inverse kinematics determines the joint angles. $,\theta_2, \theta_3, \theta_4, \theta_5, \theta_6, \theta_7, \theta_8$ (for details see (Iossifidis, 2013)).

Constraints for the Redundancy Circle. The redundancy angle α spans all redundant arm configurations consistent with the same tool position and orientation. The rate of change of the redundancy angle generates self-motion, which can be used to accommodate the two additional constraints of obstacle avoidance for the upper arm and joint limits at the wrist. To do that, we must compute which sectors on the redundancy circle is prohibited forbidden by these constraints.

Any obstacle o_i, that reaches up to the elbow, defines a to-be-avoided segment on the redundancy circle centered on κ_i and with an angular range of σ_i (see Fig. 5) Transforming limitations of joint angle range into constraints on the redundancy circle is more complicated. The most important joint angle limitation concerns the wrist, where the lower arm and the hand are spatially aligned. The angle μ between the hand q_h and the forearm q_f must be larger than $\pi/2$, which is true as long as

$$-(\pi - \mu) \leq \theta_8 \leq \pi - \mu. \qquad (6)$$

Fig. 5 illustrates that this can be used to compute the corresponding allowed sector on the redundancy circle.

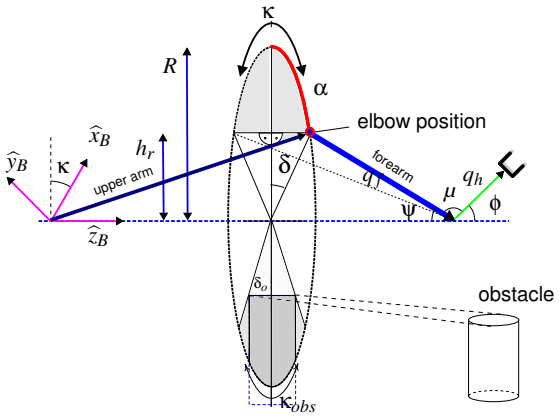

Figure 5: Geometrical construction to avoid joint configurations at the wrist and an obstacle reaching into the redundancy circle defines a to-be-avoided angular segment of that circle.

Figure 6: Null space motion of the elbow while the end effector is moving towards the target.

To do that, define a coordinate system the z'-axis of which is aligned with the shoulder-wrist-axis of the robot arm. If ϕ_w and θ_w describe the azimuth and elevation of the wrist, then the transformed hand vector, q'_h is:

$$q'_h = \mathcal{R}_y^{-\theta_w} \mathcal{R}_z^{-\phi_w} q_h \tag{7}$$

After the transformation, the redundancy circle lies in a plane parallel to the $x'y'$-plane, so that we may project q'_h onto that plane to obtain:

$$\kappa = \arctan(q_h^{y'}, q_h^{x'}) \tag{8}$$

as the center of the prohibited sector of the redundancy circle. The angular extent of the prohibited region $\kappa \pm \delta$ follows from equation 6:

$$\delta = \arccos(h_r / r) \tag{9}$$

where h_r, ψ, c and ϕ are auxiliary quantities, which can be derived from figure 5:

$$h_r = c \cdot \tan(\psi) \tag{10}$$

$$c = |q_w| - |q_m| \tag{11}$$

$$\psi = \pi - (\mu + \phi) \tag{12}$$

$$\phi = \arccos\left(q_h^{z'} / |q_h'|\right). \tag{13}$$

The obstacle induced prohibited region on the redundancy cycle is calculated analogous, with κ_o as the center of the prohibited region and δ_o as it's extend (figure 5).

3 IMPLEMENTATION AND RESULTS

In the previous section we described the design of the target system and the closed form solution for the inverse kinematics which is the mathematical basis for the incorporation of the contact forces measured by the artificial skin. Whereby forces detected by the artificial skin around the upper arm is interpreted as forces on the elbow and those detected by the artificial skin around the fore arm as forces on the wrist.

The input of the artificial skin around the upper arm generate a null space motion of the 7-degree-of-freedom arm (motion of the elbow along redundancy cycle (see 4)). This motion does not affect the end effector position and it's orientation and is used to satisfy motion constrained. Forces detected by the artificial skin associated with the wrist is used to move the end effector by the human operator to the desired direction during a collaborative task (figure 8).

Goal directed trajectories for the end effector in the following experiments are generated by means of the attractor dynamics approach described in (Iossifidis and Schöner, 2004; Iossifidis and Schöner, 2006).

For the demonstration of performance of the system, we conducted two experiments. In the first experiment (figure 6) we demonstrate how null space motion of the robot arm is initiated while the end effector is moving towards a target without aborting it's motion, end effector position or orientation. In figure 7 the contact force measured by the artificial skin around the wrist initiates an arm motion in the direction of the applied force. The human intuitively make use of the haptic interface in order to move the robot arm to the desired position.

In the second experiment a human user intervene in order to support the robot to avoid a collision with the obstacle that has not been detected by the vision sensor. In Fig. 8 [A] the robot arm starts its trajectory towards the small object. To avoid a collision between the elbow and an obstacle that has not been detected by the vision sensor, the human operator touches the skin on the upper cuff of the robot's arm ([B] - [C]), in order to force the robot to lift its elbow. The system detects the force, determines its magnitude and cal-

Figure 7: Human operator pushes the wrist of the robot to free the workspace.

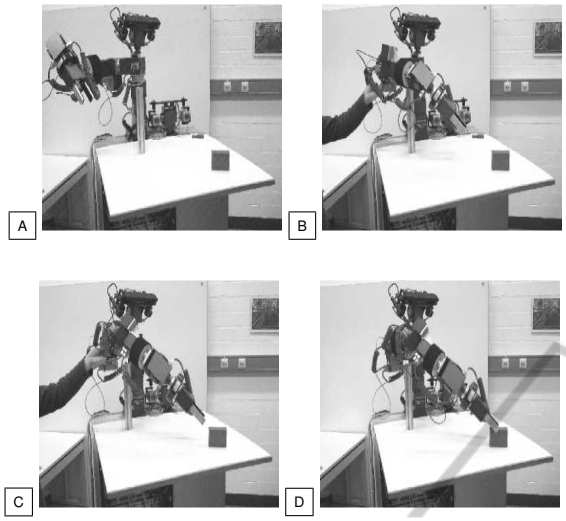

Figure 8: The human operator initiate a motion of the elbow upward by touching the skin and helps the robot to avoid a collision with the obstacle.

culates the force-direction with respect to the current arm posture. On the basis of this estimate the robot starts (B) its elbow-movement in the direction of the detected force. In A - D the robot moves its elbow without changing the intended trajectory of the end-effector. In D the robot completes its trajectory and grasps the object.

4 CONCLUSIONS

The presented work addressed and clarify the relation between safety aspects and intuitive direct physical interaction in collaborative working situations involving man and robotic assistant systems. An haptic interface was introduction able to cover arbitrary robotic structures and providing the functionality of an artificial skin. The cylindric cuffs covered by the artificial skin transformed the scalar valued measurements into a vector valued force which was fed into the motion generation scheme. For the robotic system we proposed an anthropomorphic design with an redundant manipulator allowing us to satisfy simultaneously motion constraints and occurring requests by the human operator.

This led to an system with a bidirectional physical interaction channel providing intuitiv and flexible interrelationship between man and machine and safety for both. The approach is implemented on the anthropomorphic robot CORA and evaluated in multiple experiments.

REFERENCES

Hollerbach, J. (1984). Optimum kinematic design for a seven degree of freedom manipulator. In *2nd Int. Symp. Robotics Research*, pages 215 –222.

Iossifidis, I. (2013). Motion constraint satisfaction by means of closed form solution for redundant robot arms. In *Proc. IEEE/RSJ International Conference on Robotics and Biomimetics (Ro-Bio2013)*.

Iossifidis, I., Bruckhoff, C., Theis, C., Grote, C., Faubel, C., and Schöner, G. (2002). CORA: An anthropomorphic robot assistant for human environment. In Proceedings. *11th IEEE International Workshop on Robot and Human Interactive Communication*, pages 392–398. IEEE.

Iossifidis, I. and Schöner, G. (2004). Autonomous reaching and obstacle avoidance with the anthropomorphic arm of a robotic assistant using the attractor dynamics approach. In *Proc. IEEE International Conference on Robotics and Automation* ICRA '04, volume 5, pages 4295—- 4300 Vol.5.

Iossifidis, I. and Schöner, G. (2006). Dynamical Systems Approach for the Autonomous Avoidance of Obstacles and Joint-limits for an Redundant Robot Arm. In *2006 IEEE/RSJ International Conference on Intelligent Robots and Systems*, pages 580–585. IEEE.

Kreutz-Delgado, K., Long, M., and Seraji, H. (1990). Kinematic analysis of 7 DOF anthropomorphic arms. In *Robotics and Automation*, 1990. *Proceedings., 1990 IEEE International Conference on*, pages 824 – 830.

Murray, R., Li, Z., and Sastry, S. (1994). *A mathematical introduction to robotic manipulation*. CRC Press.